



ISSN: 0976-3031

Available Online at <http://www.recentscientific.com>

CODEN: IJRSFP (USA)

*International Journal of Recent Scientific Research*  
Vol. 8, Issue, 9, pp. 20425-20432, September, 2017

**International Journal of  
Recent Scientific  
Research**

DOI: 10.24327/IJRSR

## Research Article

# PHOTOCATALYTIC ACTIVITY OF GEL/CDS/PVA NANOCOMPOSITES FOR DEGRADATION OF DYE UNDER SOLAR LIGHT IRRADIATION

Mshari Ayad Alotaibi\*

Department of Chemistry, College of Science and Humanities, Prince Sattam Bin Abdulaziz University, Alkharj, Kingdom of Saudi Arabia

DOI: <http://dx.doi.org/10.24327/ijrsr.2017.0809.0892>

### ARTICLE INFO

#### Article History:

Received 20<sup>th</sup> June, 2017  
Received in revised form 29<sup>th</sup> July, 2017  
Accepted 30<sup>th</sup> August, 2017  
Published online 28<sup>th</sup> September, 2017

#### Key Words:

CdS nanocomposite; Photocatalysis; Rhodamine B; degradation; Gamma radiation

### ABSTRACT

Photocatalytic degradation of Rhodamine B (RhB) was studied using the photocatalyst GEL/CdS/PVANCs under solar light irradiation. The crosslinked GEL/CdS/PVANCs catalyst was prepared by using gamma irradiation as initiator. Glutaraldehyde (0.5% v/v) was incorporated after irradiation to crosslink the gelatin chains. The prepared photocatalyst was characterized by an infrared spectrophotometer (IR), X-ray diffraction (XRD), transmission electron microscope (TEM) and ultraviolet-visible (UV-Vis) spectroscopy. The photocatalytic activities of the composites were investigated by the degradation of Rhodamine B (RhB) as a standard dye. The factors affecting the adsorption capacity of RhB onto GEL/CdS/PVANCs, such as catalyst concentration, RhB concentration and reaction pH on degradation were investigated. The degradation efficiency of RhB increased as pH increased upto pH 10. Then started decreasing at pH values higher than pH 10. It was verified that the RhB degradation rate fits a pseudo-first-order kinetics of the GEL/CdS/PVANCs amount. The degradation kinetics was fitted to fit well Langmuir-Hinshelwood rate law.

Copyright © Mshari Ayad Alotaibi, 2017, this is an open-access article distributed under the terms of the Creative Commons Attribution License, which permits unrestricted use, distribution and reproduction in any medium, provided the original work is properly cited.

## INTRODUCTION

In both developing and industrialized countries, a growing number of organic pollutants are discharged into all kinds of open waters [1]. Among those organic pollutants, soluble organic dyes are one of the major groups of pollutants in the wastewater. Organic dyes used in textile and food industries are their important sources of the environmental contaminations due to their non biodegradability and high toxicity to aquatic creatures and carcinogenic effects on humans. Hence, removal of dyes. From such waste waters is a major environmental problem and complete dye removal is necessary because dyes will be visible even at low concentrations[2].

Rhodamine B (RhB) is an important dye, which is widely used in textile, printing, paper, pharmaceutical and food industries[3]. It causes carcinogenic and teratogenic effects on public health[4]. Also, causes irritation to skin, eyes and respiratory tract. It is also a well-known water tracer fluorescent. In recent years, there are many research works[5-7] focusing on the degradation mechanism of RhB, most of them concerned the mechanism under visible illumination, and N-deethylation of RhB was the main degradation mechanism. Therefore, the control against dye wastewater pollution is an important issue to tackle throughout the world.

"Photocatalytic degradation of organic pollutants using semiconductor photocatalysts has attracted considerable amount of research interests because It is considered a potential solution to solve environmental pollution[7]. Consequently, the design and development of the efficiency of photocatalysts is the key issue and main challenge for the degradation of organic pollutants."The photocatalytic oxidation is one of the emerging technologies for the elimination of organic micropollutants because of the efficiency in their mineralization, ideally producing as end products CO<sub>2</sub>, H<sub>2</sub>O, and inorganic mineral ions[8],[9],[10]. Among them, photocatalytic degradation has attracted widespread attention due to its low cost, simplicity, high efficiency, and low secondary pollution. Photocatalysis has been an active area of research for several years owing to its potential application in water decontamination and hydrogen production[10]. In recent years, semiconductor photocatalysts have a promising potential to utilize solar energy to solve many related problems, such as organic pollutants degradation and H<sub>2</sub> production from water splitting [11],[12].

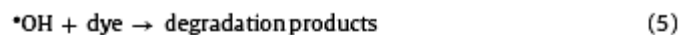
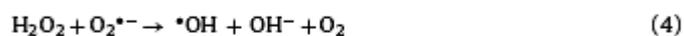
Cadmium sulfide (CdS), as an n-type semiconductor, has been attracting increasing attention as a visible-light catalyst due to its narrow band gap at 2.42 eV (512nm) [13],[14]. CdS has been regarded as a promising photocatalytic water-splitting

\*Corresponding author: Mshari Ayad Alotaibi

Department of Chemistry, College of Science and Humanities, Prince Sattam Bin Abdulaziz University, Alkharj, Kingdom of Saudi Arabia

visible-light photocatalyst, but there exist some problems in the use of CdS nanoparticles including photocorrosion and higher toxicity [15]. It is well known that CdS undergo photocorrosion upon irradiation because of oxidizing holes which cause semiconductor decomposition into sulfur and metal ions[16]. Therefore, it is absolutely vital to develop a suitable method to solve the above two problems of this material. Recently, several attempts have been made to address the above two problems and this is a very active topic of research in CdS photocatalysis[15]. At the same time, the used up catalyst suspensions in slurry need centrifugation that is expensive in terms of time and reagents. So, it is still a great challenge to immobilize powdery photocatalysts by a facile, economical and effective method. Currently, a radiation synthesis method is widely used as a facility and efficient method for the synthesis of nanocomposites with different photocatalysts on different carriers owing to its recyclability, simple operation and low cost. Thus, a radiation synthesis method to obtain recyclable CdS nanocomposites with high photocatalytic activity is highly desirable.

Recently, some groups have reported the preparation of the nanocomposites using gamma ray irradiation[17],[18]. There are many advantages in using gamma ray radiation, such as no need to use initiators, cross linking agents, or other auxiliary substances. This helps to reduce costs, makes the technology simple, does not lead to byproducts and waste, and lead to the production is of high purity products[19]. Many researchers have focused on further improving the photoactivities and photostabilities of CdS. One of the approaches is to combine CdS with supporting materials to accelerate the charge separation and migration in the photocatalytic procedure [20],[21]. Fu *et al.* [22], prepared CdS/RGO nanocomposites using gamma ray irradiation-induced reduction method and evaluated for the photocatalytic degradation of Rhodamine B. The prepared CdS/RGO nanocomposites under dose of 300 kGy and containing 83.4 wt % CdS demonstrated good photocatalytic performance for Rhodamine B with a degradation efficiency of 93% under visible light. Makama *et al.* [23] reported visible light active CdS/TiO<sub>2</sub> nanocomposites containing various CdS content were successfully synthesized using microwave-assisted hydrothermal synthesis. The photocatalytic activities of the samples were studied using methylene blue as a model pollutant. Han *et al.* [24] produced a ternary hierarchical nanostructure, CdS-1D ZnO-2D GR, made up of CdS-sensitized 1D ZnO nanorod arrays on a 2D graphene (GR) sheet, which served as an efficient visible-light-driven photocatalyst. Such novel materials and the fact that they were synthesized at low temperature open up new opportunities for designing highly effective and sought after solar driven photocatalysts. Mechanistically, CdS photocatalyst is first evoked by relevant light and subsequently initiates the photodegradation of contaminants. At first, CdS photocatalyst is first evoked by relevant light to create electrons. The electrons are then scavenged by molecular oxygen O<sub>2</sub> to yield the superoxide radical anion O<sub>2</sub><sup>•-</sup> (Eq. (2)) and hydrogen peroxide H<sub>2</sub>O<sub>2</sub> (Eq. (3)) in oxygen-equilibrated media. These new formed intermediates can interact to produce hydroxyl radical <sup>•</sup>OH (Eq. (4)). It is well known that the <sup>•</sup>OH radical is a powerful oxidizing agent capable of degrading most pollutants (Eq. (5)) [25]:



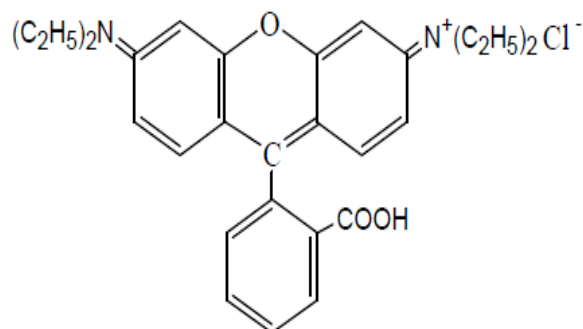
In this research, GEL/CdS/PVANCS has been synthesized by initiating the polymerization reaction by gamma-ray irradiation. Our aim of this study is to examine the photocatalytic process of the Rhodamine B dye under solar irradiation

## Experimental

### Materials

Gelatin (GEL) (Sigma–Aldrich Company) and polyvinyl alcohol (PVA), of purity 99% (Merck, Germany) were used as received. CdCl<sub>2</sub>, sodium thiosulfate (Na<sub>2</sub>S<sub>2</sub>O<sub>3</sub>·5H<sub>2</sub>O), were purchased from Aladdin.

The dye used in the experiments was Rhodamine B (RhB) (λ<sub>max</sub> = 554 nm). This dye is depicted in Chart 1. The dye was commercial grade and was used without any further purification. The other chemicals were reagent grade and used as received. The structure of the RhB dye is shown below:



### Synthesis of Gelatin/CdS/PVA nanocomposites (GEL/CdS/PVANCS)

In a typical method, GEL/CdS/PVANCS were prepared according to the method reported in previous work by Ghosh *et.al* [26]. Particularly, at first, 0.3 g of gelatin was dissolved in 30 ml of distilled water to make a 3% aqueous solution under ultrasonic stirring for 1.5 h at room temperature. A 5-ml aliquot of CdCl<sub>2</sub> stock solution (2.0 mM) in water was added to 10 ml of gelatin solution and vigorously stirred for 10 min, subsequently, an appropriate amount of freshly prepared aqueous solution of sodium thiosulfate (10 ml, 1.2 M). Subsequently, 10 ml of PVA (10 wt%) was added to the mixed suspension solution and the mixture was dispersed with ultrasonic, at room temperature for 60 min. The reaction mixture was purged with nitrogen for 8–10 min to expel oxygen from the reaction mixture and irradiated in Co<sup>60</sup> gamma ray cell 220 ( nordion INT-INC, Intario, Canada) facility of King Abdulaziz City for Science and Technology (KACST), Riyadh, Kingdom of Saudi Arabia. The polymerization was carried out at 30 kGy at a dose rate of 1.2 kGy/h. After

irradiation, samples were immersed in glutaraldehyde (0.5% v/v) solution for 6 h.

The  $S^{2-}$  ion was combined with  $Cd^{2+}$  chelated in crosslinked composite to form yellow CdS nanocrystals. The composite turned color from a chromaticity to yellow, indicating the successful formation of CdS nanocrystals in the nanocomposite. After the reaction was completed, the resulting nanocomposite was washed with absolute ethanol and double distilled water for three times, respectively, and dried in air atmosphere in an oven at 50 °C.

### Characterization

Absorption spectral measurements were carried out with Shimadzu UV-2450 UV- visible spectrophotometer.

FT-IR spectra were recorded on Mattson 1000, Unicam infrared spectrophotometer Cambridge, England in the range from 400–4000  $cm^{-1}$  using KBr pellets.

X-ray diffraction patterns were obtained with XD-DI Series, Shimadzu apparatus using nickel-filtered and Cu-K $\alpha$  radiation ( $\lambda = 1.54056\text{\AA}$ ).

Scanning electron microscope-Japan), with an energy dispersive spectroscopy (EDS) X-ray spectrometer. For TEM measurement samples were grounded and suspended in ethanol, and a drop of the resultant mixture was deposited on an ultra thin, carbon-supported Cu grid, and air-dried. Energy-filtered electron powder diffraction used TEM JEOL: JEM-100cx.

### RhB adsorption isotherms

In the batch adsorption experiments, 20 mg of photocatalyst and 50 ml of RhB solution with varied initial concentrations was added into 100 ml flasks, which were shaken at 25°C for 120 min. After the photocatalyst particles were removed by centrifugation, the residual concentration of RhB was determined spectrophotometrically at  $\lambda = 554$  nm. The  $q_e$  of photocatalyst for RB were calculated by below Eq.:

$$q_e = \frac{(C_0 - C_e)V}{W}$$

where  $q_e$  is the amount of dye adsorbed per unit mass of adsorbent (mg/g).  $C_0$  and  $C_e$  are initial concentration and the equilibrium concentration (mg/l), respectively,  $V$  (l) is the volume of the RhB solutions and  $W$  (g) is the weight of the photocatalyst.

### Photocatalytic degradation studies

The visible light photo catalytic performance of the GEL/CdS/PVANCs were estimated for the degradation of Rh.B as model pollutant dyes and the rates of degradation were calculated.

A 20 mg of the GEL/CdS/PVANCs was suspended in 100 ml of RhB solution (25  $mg\ l^{-1}$ ), then irradiated under solar light. Prior to irradiation, the reaction mixture was stirred in the dark for 1 hour to reach the adsorption/desorption equilibrium. After equilibrium, the RhB concentration (non-adsorbed) was detected and taken as initial concentration for photocatalytic process. After that, it was irradiated with sunlight.

At periodic intervals, about 5 ml was withdrawn and the extent of degradation was then analyzed by spectrophotometer at 554

nm. The experimental studies were carried out by varying concentrations of RhD within a range of 25–150 ppm. The photodegradation rate for each experiment is calculated using the following equation (2):

$$\text{photodegradation rate} = (C_0 - C/C_0) \times 100 \quad (2)$$

where,  $C_0$  the concentration of RhB before illumination and  $C$  the concentration of RhB in suspension after time  $t$  ( $mg\ l^{-1}$ ). The total uncertainty for all experiments ranged from 3–5%.

## RESULTS AND DISCUSSION

### Characterization of GEL/CdS/PVANCs

In order to examine the differences between GEL/CdS /PVA and GEL/PVA, the FTIR spectra were applied to the study. The FTIR spectrum of GEL/CdS /PVA (Fig. 1b) showed many of the changes from that of GEL/PVA (Fig. 1a). The wide peak at  $3365\text{cm}^{-1}$ , corresponding to the stretching vibration -OH, -NH $_2$  and -CONH groups, shift to  $3325\text{cm}^{-1}$  and became broader and stronger, which indicated the strong interaction between these groups and CdS [27]. The peak at  $405\text{cm}^{-1}$  corresponded to the characteristic peak of CdS. Also, the spectrum of GEL/CdS /PVA showed the disappearance of the band at  $1595\text{cm}^{-1}$  and the buildup of the band at  $1656\text{cm}^{-1}$ , which might relate to the consumption of -NH $_2$  groups, as a result of the crosslinking process and the complexation [25]. The FTIR spectrum of the GEL/PVA showed the peak around  $3400\text{cm}^{-1}$  indicates the presence of O-H group with polymeric association and a secondary amide. The peak at  $1728\text{cm}^{-1}$ , indicate the esterification of PVA and gelatin. This is in agreement with Dharmendra *et al.* [28].

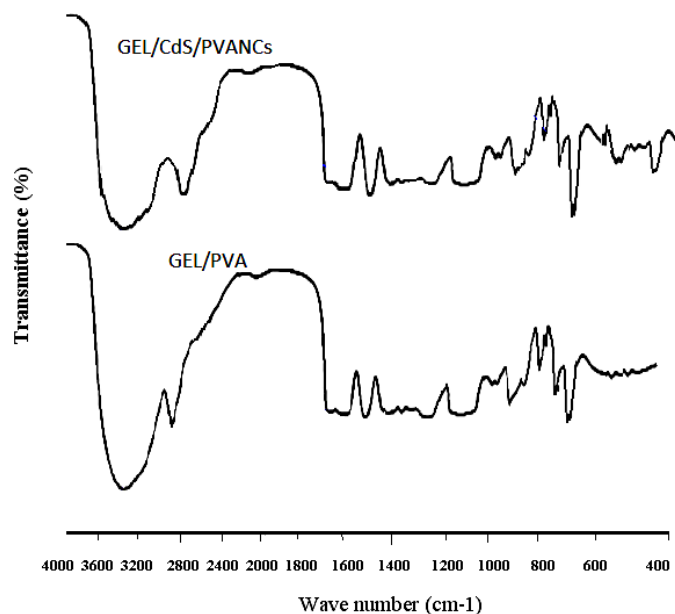


Fig 1 FTIR spectra of GEL /PVA and GEL/CdS/PVANCs.

TEM image of the GEL/CdS/PVANCs (Fig. 2) indicate CdS particle disperse well and the average size of CdS nanoparticles is ~ 10-15 nm.

The nanoparticles are randomly distributed and their particulars are not equally uniform throughout the matrix.

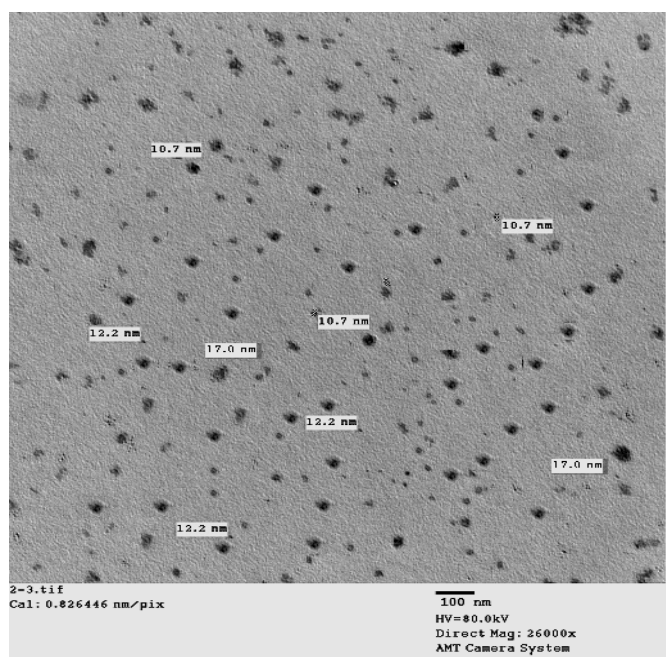


Fig 2 TEM micrograph of GEL/CdS/PVANCs

Fig. 3 shows the EDS spectrum of the GEL/CdS/PVANCs. The presence of Cd and S peaks confirmed the successful formation of CdS nanostructures.

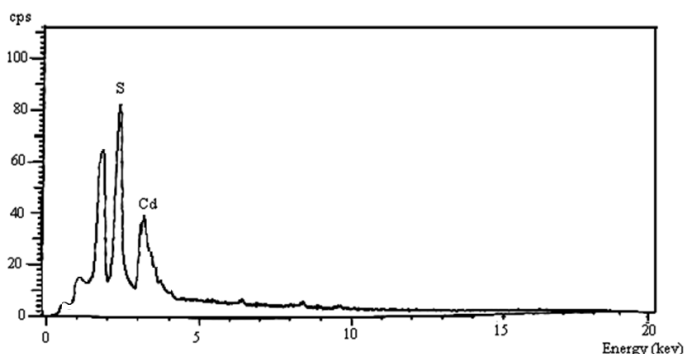


Fig 3 EDX spectra of GEL/CdS/PVANCs.

XRD patterns of pure GEL/PVA and GEL/CdS/PVANCs are shown in Fig.4, indicating the existence of CdS particles. The XRD pattern of GEL//PVA (Fig. 4a) revealed the characteristic peak at  $2\theta = 20.43^\circ$ , which agree with the pattern of the hydrate polymorph of GEL/PVA reported previously[29]. The XRD patterns for GEL/CdS/PVANCs (Fig.4b) exhibited the additional peaks at  $2\theta = 27.081^\circ$  (111),  $45.4^\circ$  (220), and  $52.6^\circ$  (311), which is an agreement with the cubic phase of CdS (JCPDS 75-1546), respectively [30], which also indicated that the cubic CdS nanocrystal structure was formed successfully in the GEL/CdS/PVANCs.

The crystallite size (D) of CDs, crystals were calculated from the Debye-Scherrer equation [31]:

$$D = K\lambda/(\beta\cos\theta)$$

where  $\lambda \rightarrow$  wavelength of Cu  $K\alpha$  line ( $\lambda = 1.5406 \text{ \AA}$ ),  $\theta \rightarrow$  diffraction angle (in radian) of the considered diffraction peak,  $\beta$  is the full-width at half maximum intensity and K is a

Scherrer constant taken as 0.90 for the almost spherical particles.

The crystallite size as calculated from Scherrer equation was found to be around 8-10 nm. Obviously, the size calculated from XRD results is smaller than observed from TEM micrograph.

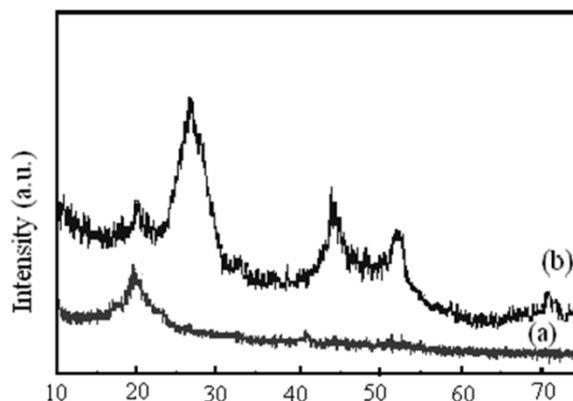


Fig 4 XRD patterns of (a) GEL/PVA and (b) GEL/CdS/PVANCs.

### Photocatalytic degradation of RhB

#### Photocatalytic activity

The photocatalytic efficiency of GEL/CdS/PVANCs were evaluated by the degradation of RhB in aqueous solutions at three different experimental conditions, and showed in Fig. 5. It can be seen that, almost no RhB photodegradation for two cases: (i) for the mixture of RhB and water in as-mixed state and (ii) when the irradiation was carried out in the absence of GEL/CdS/PVANCs at 4 hours. These results indicate that the absence of RhB degradation in such mixtures. In non irradiated suspensions, almost insignificant degradation of the RhB was observed with only 6.95%, due to adsorption of RhB molecules onto GEL/CdS/PVANCs [9]. Also, it can be noted that the experiment in the absence of GEL/CdS/PVANCs showed almost no RhB degradation, implying that the self photolysis of RhB is insignificant when irradiated with visible light. However, in the presence of catalyst a rapid degradation of RhB occurred by irradiation. This result obviously indicates that the photocatalytic activity of RhB contaminate degradation is effectively enhanced in the presence of CdS.

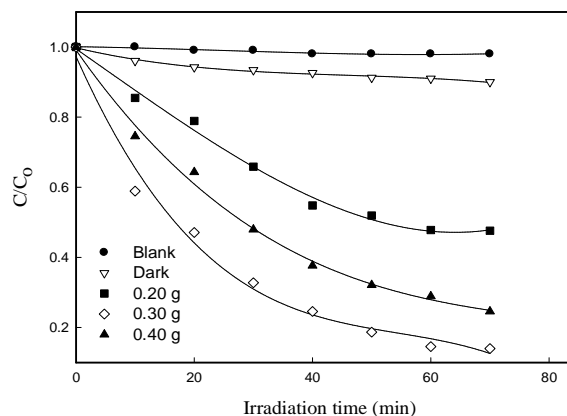


Fig 5 Visible light induced photodegradation efficiency of RhB dye at different GEL/CdS/PVANCs.

#### Effect of amount of catalyst

Photocatalyst amount is one of the critical parameters affecting the efficiency of degradation. In order to evaluate the photocatalytic activity of the amount of photocatalyst, a series of experiments were conducted where the catalyst amount varied from 0.1 to 0.40 g, at dye concentration of 25 mg/l. The results are shown in Fig. 6a. It was observed that as the amount of GEL/CdS/PVANCs was increased. Higher concentrations of photocatalyst were thought to absorb more incident photons and produce more photo generated charge carriers, up to an optimum value of dosage where the maximum photocatalytic activity was realized. But after 0.30g, there is a decrease in degradation efficient of RhB [27]. This can refer to the fact that, the solution becomes turbid and hence cause shields the light and hinder the light penetration. In addition, the photons could not be continuously injected into photocatalyst particles and may have accelerated their combination of electrons and holes [29]

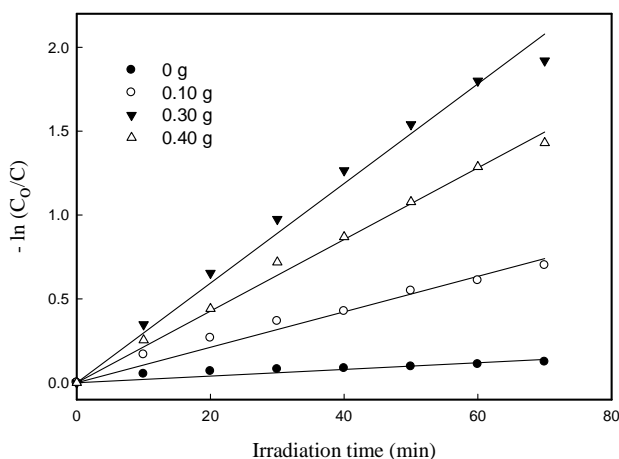
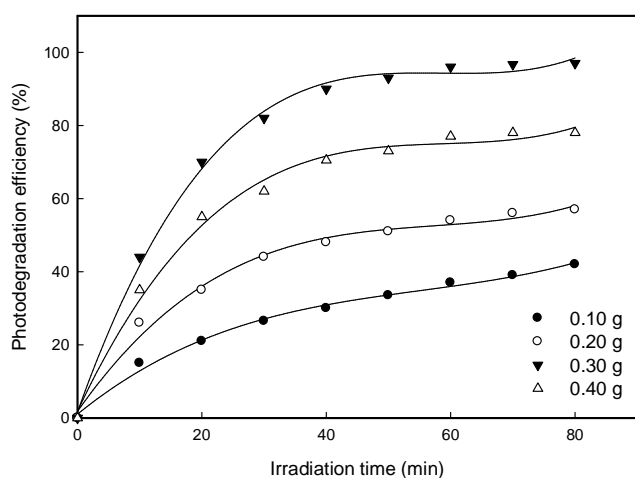


Fig 6 (a) Effect of illumination time (min) on photo-degradation efficient (%) of RhB onto GEL/CdS/PVANCs. Control: temp.: 30°C; t: 80 min at different of catalyst amount (b) first-order photo-degradation kinetics at different GEL/CdS/PVANCs.

The photocatalytic degradation of RhB follows a pseudo first order Langmuir-Hinshelwood (LH) model. At low concentrations apparent rate order can be expressed as, [32]:

$$\ln\left(\frac{C_0}{C}\right) = k_{obs} t$$

where  $C_0$  is the initial reactant concentration (mg/l) and  $t$  the illumination time (min). The apparent rate constant,  $k_{obs}$  can be taken as the apparent first order rate constant of the degradation reaction. A plot of  $\ln(C_0/C_i)$  versus  $t$  yields a slope of  $k_{obs}$ . The linear graph of  $-\ln C_0/C$  versus time (min) confirms the pseudo first order reaction for the RhB degradation. The apparent rate constant  $k_{obs}$  ( $\text{min}^{-1}$ ) increase with the increasing of the amount of catalyst dosage upto 0.30g when other parameters are kept unchanged as shown in Fig.6b. The derived apparent reaction rate constants ( $k_{obs}$ ) for the catalysts which have pseudo first-order kinetic and linear regression coefficients are summarized in Table 1. The table confirms the aforementioned interpenetrations where the increase in the amount of catalyst results in an increase in the rate of the reaction. This result can be attributed to the increase in the number of photons absorbed and the reaction rate was accelerated, and also the number of dye molecule adsorbed [30]. As shown in Table 1, the polymeric nanocomposites have higher photocatalytic activity, which is represented by the largest  $k_{obs}$  value. Table 1

Table 1 Pseudo-first order rate constants for the degradation and linear regression coefficients of the catalyst amount of GEL/CdS /PVANCs.

Catalyst	$k_{obs}$ ( $\text{min}^{-1}$ )	$R^2$
0.0 g	$1.49 \times 10^{-3}$	0.900
0.10 g	$9.54 \times 10^{-3}$	0.986
0.30 g	$2.815 \times 10^{-2}$	0.990
0.40 g	$2.052 \times 10^{-2}$	0.995

### Effect of Initial RhB Dye Concentration

Fig. 7. shows the effect of the initial RhB concentration on the photocatalytic degradation efficiency. The initial RhB concentration in this study was varied from 25-150 mg/l. It can be seen from the figure that the degradation efficiency of RhB tended to decrease with initial RhB concentration increased. Similar results have been presented for the photocatalytic oxidation of other organic compound [7],[9],[29]. A possible explanation is that the generation of  $\bullet\text{OH}$  on the catalyst surface is reduced when the initial RhB concentration is increased. More RhB dyes are adsorbed on the surface of GEL/CdS/PVANCs will make fewer active sites available for the  $\bullet\text{OH}$  adsorption.

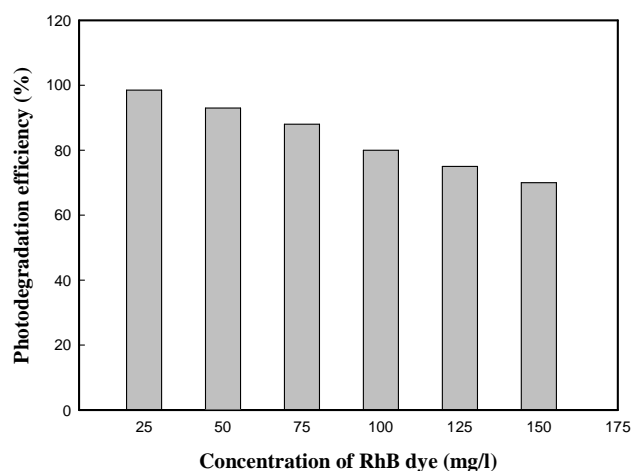


Fig 7 Effect of initial RhB concentration on the photodegradation efficiency (catalyst amount = 0.1 g/100 ml).

Also, the solution transmittance decreased, resulting in fewer photons reaching the GEL/CdS/PVANCs surface to activate it to generate hydroxyl  $\cdot\text{OH}$  and  $\text{O}_2^{\cdot-}$  radicals. Hence, large amounts of adsorbed RhB would have an inhibitory influence on the reaction between RhB molecules and hydroxyl radicals due to the lack of any direct contact between them.

### Effect of pH

"pH An important parameter in the photocatalytic reactions taking place on the particulate surfaces is the pH of the solution, since it governs the surface charge properties of the photocatalyst and size of aggregates it forms" [9]. The effect of pH was carried out at different pH values (in the range 3 - 12) at dye concentration (25 mg/l) are shown in Fig. 8. It can be seen from the figure that the degradation efficiency of RhB increased as pH increased upto pH 10 after this value resulted in a decrease.

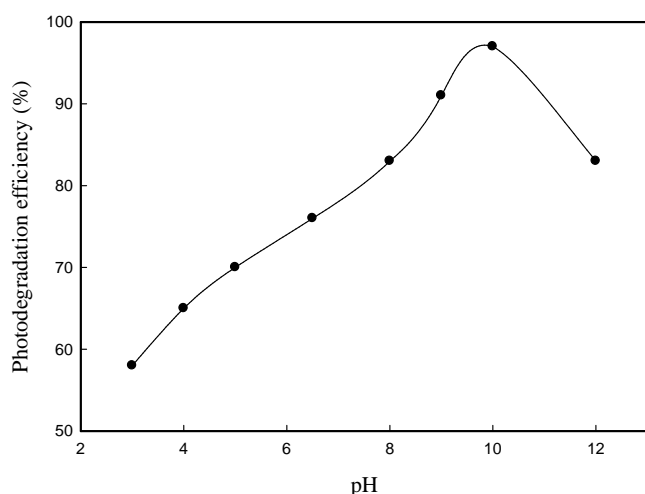


Fig 8 Effect of pH on the photodegradation efficiency (%) of RhB dye onto GEL/CdS/PVANCs. (Conc.: 25 mg/l; temp.: 30 °C; t: 4 h).

The variation is not due to any change in the absorption of light as the  $\lambda_{\text{max}}$  for the dye changes very little (551-553 nm) in the pH range of 3-12 even though rhodamine exists in two principal forms in water, i.e. cationic ( $\text{RhB}^+$ ) or zwitter ionic ( $\text{RhB}^{\pm}$ ) [33]. In the acidic range the dye will be in cationic form ( $\text{RhB}^+$ ). Thus, electrostatic repulsion may occur between RhB and the catalysts, resulting in the decrease of the degradation efficiency. At higher pH value, the  $\text{RhB}^+$  gets deprotonated and its Zwitter ion is formed. In addition, alkaline pH conditions can help in the production of  $\cdot\text{OH}$  radicals, which assists in the degradation through  $\cdot\text{OH}$  radical oxidation mechanism. All of these can promote the degradation of RhB and the reaction intermediates. Above pH 10, the catalyst surface may be covered by  $\text{OH}^-$  ions and hence it is negatively charged. Since RhB is not protonated above pH 10 it will be repelled by the negatively charged surface of catalysis. Hence, the degradation efficient decreased above pH 10.

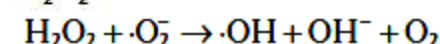
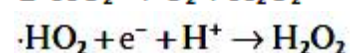
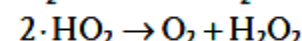
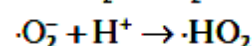
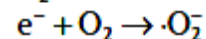
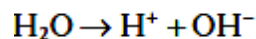
### Photocatalytic reaction mechanism

"The use of composite materials is a technique used to reduce the hole-electron pair recombination induced by the photocatalytic processes. Materials such as metals, metal oxides and organic molecules can be used for these purposes [34], [35]. In the presence of air or oxygen, the irradiated

semiconductor nanocomposites are capable of destroying many organic contaminants. On the surface of the CdS is activated by a photon of light ( $h\nu$ ) and produces electron-hole pairs which are strong oxidizing and reducing agents: "



Most of the photo-generated electrons and holes react with  $\text{H}_2\text{O}$  and oxygen  $\text{O}_2$  [36], [37].



It is well known that the  $\cdot\text{OH}$  radical is a powerful oxidizing agent capable of degrading most pollutants. The presence of  $\text{O}_2$  can prevent the re-combination of hole-electron pairs. Successive reactions let the oxidation of the RhB and the complete photodegradation. Normally, RhB was found to be very stable under solar light irradiation in the absence of catalysts. "According to some investigations one possible mechanism for the degradation of RhB is composed of three main steps are involved. They are (1) N-deethylation, (2) cleavage of the chromophore, (3) mineralization of dye" [7], [35],[38].

The photostability and reusability of GEL/CdS/PVANCs were further studied by collecting and reusing the photocatalyst for five cycles. The results revealed that the catalytic activity of the used catalyst shows nearly 96 % repeatability in the first 2 cycles and minor drops of 13 % of activity upto 3 cycles. This result proves that the catalyst has an excellent stability and great potential application.

### CONCLUSIONS

The above studies demonstrate that the gamma irradiation technique can be used to prepare GEL/CdS/PVANCs and can efficiently catalyze the degradation of RhB dye in the presence of sunlight. The reaction rates of photocatalytic degradation of RhB were influenced by pH values, which could affect the surface characteristics of GEL/CdS/PVANCs and the distribution of reactive species. High photocatalytic activity was observed with a medium pH of 10. The photocatalytic degradation of RhB dye decreased as the initial RhB dye concentration increased. The photocatalytic degradation of RhB in aqueous GEL/CdS/PVANCs follows a pseudo-first-order kinetics. Moreover, comparison studies revealed that the Gel/CdS/PVANCs had a higher photocatalytic efficiency than pure CdS. This study presents a low cost, green, rapid, and a simple procedure for the degradation of dye pollutants in aqueous wastewater solutions.

## Acknowledgments

The author would like to thank prof. Manal Abou Taleb for valuable discussions and insights. thank you and looking to receive the final draft soon

## Reference

1. M.A. Shannon, P.W. Bohn, M. Elimelech, J.G. Georgiadis, B.J. Mariñas, A.M. Mayes, Science and technology for water purification in the coming decades, *Nature*. 452 (2008) 301-310. doi:10.1038/nature06599.
2. A.M. S. Papić, N. Koprivanac, A.L. Božić, Removal of some reactive dyes from synthetic wastewater by combined Al(III) coagulation/carbon adsorption process Dyes, *Pigments*. 62 (2004) 291-298.
3. S. Daniel, S.U. S, Synthesis, characterization and adsorption behaviour of MgO nano particles on Rhodamine B dye, *J. Chem. Pharm. Res.* 7 (2015) 713–723. <http://www.jocpr.com/articles/synthesis-characterization-and-adsorption-behaviour-of-mgo-nano-particles-on-rhodamine-b-dye.pdf> (accessed March 14, 2017).
4. V.K. Gupta, Suhas, Application of low-cost adsorbents for dye removal - A review, *J. Environ. Manage.* 90 (2009) 2313-2342. doi:10.1016/j.jenvman.2008.11.017.
5. M. Cotto-Maldonado, Photocatalytic Degradation of Rhodamine-B Under UV-Visible Light Irradiation Using Different Nanostructured Catalysts., *Am. Chem. Sci. J.* 3 (2013) 178–202. <http://search.ebscohost.com/login.aspx?direct=true&profile=ehost&scope=site&authtype=crawler&jrnl=22490205&AN=90543563&h=nDAsUR4a/oakTZ4Vz0FlkvMjKrVnymMt3DmREMRlcEeilmlM39esfIvv05M3bwf+V5mzGf/WG8SNUEYLMGQSyA=&cl=c>.
6. S. Rajalakshmi, S. Pitchaimuthu, N. Kannan, P. Velusamy, Enhanced photocatalytic activity of metal oxides/ $\beta$ -cyclodextrin nanocomposites for decoloration of Rhodamine B dye under solar light irradiation, *Appl. Water Sci.* (2014). doi:10.1007/s13201-014-0223-5.
7. Y. Tang, X. Liu, C. Ma, M. Zhou, P. Huo, L. Yu, *et al.*, Enhanced photocatalytic degradation of tetracycline antibiotics by reduced graphene oxide–CdS/ZnS heterostructure photocatalysts, *New J. Chem.* 39 (2015) 5150–5160. doi:10.1039/C5NJ00681C.
8. [8]S. Qourzal, N. Barka, M. Tamimi, A. Assabbane, Y. Ait-Ichou, Photodegradation of 2-naphthol in water by artificial light illumination using TiO<sub>2</sub> photocatalyst: Identification of intermediates and the reaction pathway, *Appl. Catal. A Gen.* 334 (2008) 386-393. doi:10.1016/j.apcata.2007.09.034.
9. M.F.A. Taleb, Adsorption and photocatalytic degradation of 2-CP in wastewater onto CS/CoFe<sub>2</sub>O<sub>4</sub> nanocomposite synthesized using gamma radiation., *Carbohydr. Polym.* 114 (2014) 65-72. doi:10.1016/j.carbpol.2014.07.061.
10. B. Palanisamy, C.M. Babu, B. Sundaravel, S. Anandan, V. Murugesan, Sol-gel synthesis of mesoporous mixed Fe<sub>2</sub>O<sub>3</sub>/TiO<sub>2</sub> photocatalyst: Application for degradation of 4-chlorophenol, *J. Hazard. Mater.* 252-253 (2013) 233-242. doi:10.1016/j.jhazmat.2013.02.060.
11. J.Y. and M.J. Shengwei Liu, Tunable Photocatalytic Selectivity of Hollow TiO<sub>2</sub> Microspheres Composed of Anatase Polyhedra with Exposed {001} Facets, *J. Am. Chem. Soc.* 132 (2010) 11914-11916.
12. Y. Xie, S. Zhang, B. Pan, L. Lv, W. Zhang, Effect of CdS distribution on the photocatalytic performance of resin-CdS nanocomposites, *Chem. Eng. J.* 174 (2011) 351-356. doi:10.1016/j.cej.2011.09.006.
13. Q. Li, B. Guo, J. Yu, J. Ran, B. Zhang, H. Yan, *et al.*, Highly Efficient Visible-Light-Driven Photocatalytic Hydrogen Production of CdS-Cluster-Decorated Graphene Nanosheets, *J. Am. Chem. Soc.* 133 (2011) 10878-10884. doi:10.1021/ja2025454.
14. M. Shang, W. Wang, S. Sun, J. Ren, L. Zhou, L. Zhang, Efficient Visible Light-Induced Photocatalytic Degradation of Contaminant by Spindle-like PANI/BiVO<sub>4</sub>, *J. Phys. Chem. C.* 113 (2009) 20228-20233. doi:10.1021/jp9067729.
15. Y. Chen, F. Li, W. Cao, T. Li, Preparation of recyclable CdS photocatalytic and superhydrophobic films with photostability by using a screen-printing technique, *J. Mater. Chem. A.* 3 (2015) 16934-16940. doi:10.1039/C5TA04065E.
16. K.P. Acharya, R.S. Khnayzer, T. O'Connor, G. Diederich, M. Kirsanova, A. Klinkova, *et al.*, Correction to The Role of Hole Localization in Sacrificial Hydrogen Production by Semiconductor-Metal Heterostructured Nanocrystals, *Nano Lett.* 12 (2012) 522-522. doi:10.1021/nl204166a.
17. M.F. Abou Taleb, A. El-Trass, S. El-Sigeny, Synthesis of polyamidoamine dendrimer (PAMAM/CuS/AA) nanocomposite and its application in the removal of Isma acid fast yellow G Dye, *Polym. Adv. Technol.* 26 (2015) 994-1002. doi:10.1002/pat.3517.
18. A.A. Al-Kahtani, M.F. Abou Taleb, Photocatalytic degradation of Maxilon C.I. basic dye using CS/CoFe<sub>2</sub>O<sub>4</sub>/GONCs as a heterogeneous photo-Fenton catalyst prepared by gamma irradiation, *J. Hazard. Mater.* 309 (2016) 10-19. doi:10.1016/j.jhazmat.2016.01.071.
19. S. El-Sigeny, S.K. Mohamed, M.F. Abou Taleb, Radiation synthesis and characterization of styrene/acrylic acid/organophilic montmorillonite hybrid nanocomposite for sorption of dyes from aqueous solutions, *Polym. Compos.* 35 (2014) 2353-2364. doi:10.1002/pc.22902.
20. Z. Ren, J. Zhang, F.-X. Xiao, G. Xiao, Revisiting the construction of graphene–CdS nanocomposites as efficient visible-light-driven photocatalysts for selective organic transformation, *J. Mater. Chem. A.* 2 (2014) 5330. doi:10.1039/c4ta00009a.
21. Z. Yan, X. Yu, A. Han, P. Xu, P. Du, Noble-Metal-Free Ni(OH)<sub>2</sub>-Modified CdS/Reduced Graphene Oxide Nanocomposite with Enhanced Photocatalytic Activity for Hydrogen Production under Visible Light Irradiation, *J. Phys. Chem. C.* 118 (2014) 22896-22903. doi:10.1021/jp5065402.
22. X. Fu, Y. Zhang, P. Cao, H. Ma, P. Liu, L. He, *et al.*, Radiation synthesis of CdS/reduced graphene oxide nanocomposites for visible-light-driven photocatalytic degradation of organic contaminant, *Radiat. Phys. Chem.* 123 (2016) 79-86. doi:10.1016/j.radphyschem.2016.02.016.

23. A.B. Makama, A. Salmiaton, E.B. Saion, T.S.Y. Choong, N. Abdullah, Synthesis of CdS Sensitized TiO<sub>2</sub> Photocatalysts: Methylene Blue Adsorption and Enhanced Photocatalytic Activities, *Int. J. Photoenergy*. 2016 (2016) 1-14. doi:10.1155/2016/2947510.
24. C. Han, Z. Chen, N. Zhang, J.C. Colmenares, Y.-J. Xu, Hierarchically CdS Decorated 1D ZnO Nanorods-2D Graphene Hybrids: Low Temperature Synthesis and Enhanced Photocatalytic Performance, *Adv. Funct. Mater.* 25 (2015) 221-229. doi:10.1002/adfm.201402443.
25. H. Zhu, R. Jiang, L. Xiao, Y. Chang, Y. Guan, X. Li, *et al.*, Photocatalytic decolorization and degradation of Congo Red on innovative crosslinked chitosan/nano-CdS composite catalyst under visible light irradiation, *J. Hazard. Mater.* 169 (2009) 933-940. doi:10.1016/j.jhazmat.2009.04.037.
26. S. Ghosh, S.C. Bhattacharya, A. Saha, Probing of ascorbic acid by CdS/dendrimer nanocomposites: a spectroscopic investigation, *Anal. Bioanal. Chem.* 397 (2010) 1573-1582. doi:10.1007/s00216-010-3654-3.
27. Z. Li, Y. Du, Biomimic synthesis of CdS nanoparticles with enhanced luminescence, *Mater. Lett.* 57 (2003) 2480-2484. doi:10.1016/S0167-577X(02)01297-1.
28. D. Jain, E. Carvalho, A.K. Banthia, R. Banerjee, Development of polyvinyl alcohol-gelatin membranes for antibiotic delivery in the eye, *Drug Dev. Ind. Pharm.* 37 (2011) 167-177. doi:10.3109/03639045.2010.502533.
29. K. Pal, A.K. Banthia, D.K. Majumdar, Preparation and characterization of polyvinyl alcohol-gelatin hydrogel membranes for biomedical applications., *AAPS PharmSciTech.* 8 (2007) 21. doi:10.1208/pt080121.
30. X.-W. Wei, X.-J. Song, J. Xu, Y.-H. Ni, P. Zhang, Coating multi-walled carbon nanotubes with metal sulfides, *Mater. Chem. Phys.* 92 (2005) 159-163. doi:10.1016/j.matchemphys.2005.01.006.
31. R. Jenkins, R.L. (Robert L. Snyder, Introduction to X-ray powder diffractometry, John Wiley & Sons, Inc, 1996.  
<http://eu.wiley.com/WileyCDA/WileyTitle/productCd-0471513393.html> (accessed March 17, 2017).
32. Y.-X. Guo, Z.-L. Xiu, D.-J. Zhang, H. Wang, L.-X. Wang, H.-B. Xiao, Kinetics and mechanism of degradation of lithospermic acid B in aqueous solution, *J. Pharm. Biomed. Anal.* 43 (2007) 1249-1255. doi:10.1016/j.jpba.2006.10.025.
33. N. Hariprasad, S.G. Anju, E.P. Yesodharan, Y. Suguna, Sunlight induced removal of Rhodamine B from water through Semiconductor Photocatalysis: Effects of Adsorption, Reaction Conditions and Additives, *Res. J. Mater. Sci.* 1 (2013) 9-17.
34. J. Mu, B. Chen, M. Zhang, Z. Guo, P. Zhang, Z. Zhang, *et al.*, Enhancement of the visible-light photocatalytic activity of In<sub>2</sub>O<sub>3</sub>-TiO<sub>2</sub> nanofiber heteroarchitectures., *ACS Appl. Mater. Interfaces.* 4 (2012) 424-30. doi:10.1021/am201499r.
35. M. Cotto-Maldonado, Photocatalytic Degradation of Rhodamine-B Under UV-Visible Light Irradiation Using Different Nanostructured Catalysts., *Am. Chem. Sci. J.* 3 (2013) 178-202. <http://search.ebscohost.com/login.aspx?direct=true&profile=ehost&scope=site&authtype=crawler&jrnl=22490205&AN=90543563&h=nDAsUR4a/oakTZ4Vz0FlkvMjKrVnymMt3DmREMRlcEeilmlM39esflvv05M3bwf+V5mzGf/WG8SNUEYLMGQSYA=&crl=c>.
36. X. Li, C. Hu, X. Wang, Y. Xi, Photocatalytic activity of CdS nanoparticles synthesized by a facile composite molten salt method, *Appl. Surf. Sci.* 258 (2012) 4370-4376. doi:10.1016/j.apsusc.2011.12.116.
37. N. Soltani, E. Saion, W.M. Mat, M. Erfani, M. Navasery, G. Bahmanrokh, *et al.*, Applied Surface Science Enhancement of visible light photocatalytic activity of ZnS and CdS nanoparticles based on organic and inorganic coating, *Appl. Surf. Sci.* 290 (2014) 440-447. doi:10.1016/j.apsusc.2013.11.104.
38. M. Sun, D. Li, Y. Chen, W. Chen, W. Li, Y. He, *et al.*, Synthesis and Photocatalytic Activity of Calcium Antimony Oxide Hydroxide for the Degradation of Dyes in Water, *J. Phys. Chem. C.* 113 (2009) 13825-13831. doi:10.1021/jp903355a.

**How to cite this article:**

Mshari Ayad Alotaibi.2017, Photocatalytic Activity of Gel/Cds/Pva Nanocomposites For Degradation of Dye Under Solar Light Irradiation. *Int J Recent Sci Res.* 8(9), pp. 20425-20432. DOI: <http://dx.doi.org/10.24327/ijrsr.2017.0809.0892>

\*\*\*\*\*